JOURNAL OF SPACECRAFT AND ROCKETS
Vol. 31, No. 6, November–December 1994

Near-Wake Structure for a Generic Configuration of Aeroassisted Space Transfer Vehicles

Virendra K. Dogra*
ViGYAN, Inc., Hampton, Virginia 23666
and
James N. Moss† and Joseph M. Price‡
NASA Langley Research Center, Hampton, Virginia 23681

Results of a numerical study are presented for hypersonic low-density nitrogen gas flow about a 70-deg blunt cone using the direct simulation Monte Carlo method.The flow conditions simulated are attainable in existing low-density hypersonic wind tunnels; encompassing freestream Knudsen numbers of 0.03 to 0.001. Particular emphasis is given to the near-wake flow and its sensitivity to rarefaction and other parametric variations. A stable vortex forms in the near wake at and below a freestream Knudsen number of 0.01, and the size of the vortex increases with decreasing freestream Knudsen number. The base region of the flow remains in thermal nonequilibrium for all cases. There is no formation of a lip separation shock or a distinct wake shock at these rarefied conditions.

Nomenclature

A	= base area of cone, $\pi d^2/4$
C_D	= drag coefficient, $2D/\rho_\infty V_\infty^2 A$
C_f	= skin-friction coefficient, $2\tau_w/\rho_\infty V_\infty^2$
C_H	= heat-transfer coefficient, $2q/\rho_\infty V_\infty^3$
C_p	= pressure coefficient, $2p/\rho_\infty V_\infty^2$
D	= drag
d	= base diameter
d_{ref}	= molecular diameter at reference temperature
Kn	= Knudsen number, λ/d
M	= Mach number
$\mathcal{M}$	= molecular weight of N_2, $\mathcal{M} = 28.02$ g/mole
$\mathcal{N}$	= Avogadro's number, 6.02252×10^{26} particles/kg-mole
p	= pressure
R	= gas constant for N_2, 296.7 J/kg-K
R_b	= cone base radius
R_c	= corner radius
Re	= Reynolds number, $\rho V d/\mu$
Re_2	= total Reynolds number, $Re_\infty(\mu_\infty/\mu_0)$
R_n	= cone nose radius
s	= distance along the body surface measured from the stagnation point
$\bar{s}$	= temperature exponent of the coefficient of viscosity
S	= speed ratio, $V/\sqrt{2RT}$
T	= thermodynamic temperature
T_i	= internal kinetic temperature
T_{ov}	= overall kinetic temperature
T_t	= translational temperature
T_w	= surface temperature
u	= axial velocity
v	= radial velocity
V	= velocity
x	= axial distance from stagnation point measured along symmetry axis
$(x/d)_0$	= location of rear stagnation point
$(x/d)_1$	= location of wake stagnation point
y	= radial distance from symmetry axis
Γ	= gamma function
γ	= ratio of specific heats ($\gamma = 1.4$)
Δ	= size of the vortex, $(x/d)_1 - (x/d)_0$
λ	= mean free path
μ	= dynamic viscosity
ρ	= density
σ	= collision cross section
τ	= shear stress

Subscripts

0	= stagnation-chamber value
ref	= reference value
stag	= stagnation point
w	= surface values
∞	= freestream values

Received Dec. 9, 1993; revision received March 28, 1994; accepted for publication April 2, 1994.

*Research Engineer. Associate Fellow AIAA.
†Research Engineer. Fellow AIAA.
‡Research Engineer.

Introduction

MAJOR missions of the emerging aeroassisted space transfer vehicles (ASTVs) will be Mars arrival, Earth return from Mars, and Earth return from the moon. These vehicles will have three primary components: the aerobrake, the payload compartment, and the main propulsion unit. Furthermore, these vehicles will maneuver within the rarefied and generally undefined outer atmosphere rather than just passing through it. To achieve stable flight under these conditions, the constraints on the center of gravity become critical, and the placement of the payload in the near wake of the aerobrake is the only suitable way to satisfy the center-of-gravity requirement.[1] The heating rate and aerodynamic forces which can result from the interaction of the near wake with the payload compartment are major concerns because they can significantly affect the size and the shape of the payload compartment. Currently, there is a lack of experimental and numerical data for blunt-body wake flows under hypersonic rarefied flight conditions. Furthermore, for flight conditions where the forebody flow is well into the continuum regime, rarefaction effects can still be significant in the wake.

Previous studies[2–5] of the aerothermodynamics for current and projected ASTVs have mainly focused on the aerobrake. Recently, the structure of the near wake of aerobrakes in the continuum flow regime has been studied numerically using the Navier-Stokes equations.[6] It is concluded in this study that the shear-layer impingement on the payload placed in the wake can raise the local heating significantly. Although the forebody flow at moderately high altitudes may be in the continuum flow regime, expansion of this flow into the wake region can produce large local Knudsen numbers. Consequently, it becomes imperative that the problem be investigated

Table 1 Wind-tunnel conditions for experiment[a]

Case	T_0, K	P_0 bar	M_∞	ρ_∞, 10^{-5} kg/m^3	V_∞, m/s	T_∞, K	λ_∞, mm
1	1099	3.5	20.2	1.73	1502	13.3	1.569
2	1100	9.3	19.7	5.19	1502	14.0	0.529
3	1299	125.5	20.6	46.65	1633	15.0	0.0594

[a] $T_w = 300$ K.

Table 2 Flow parameters and selected results[a]

Case	Kn_∞,	S_∞	Re_∞	Re_2	C_H stag	C_D	Δ
1	0.0317	16.9	768	28.0	0.366	1.61	0.00
2	0.0107	16.5	2220	84.1	0.213	1.54	0.19
3	0.0012	17.3	20600	725.7	0.0965	1.54	0.75

[a] $d = 4.95$ cm, $R_n = 1.248$ cm, $R_c = 0.036$ cm.

with an analysis capable of properly modeling the general features of low-density flows. Such a capability exists in the direct simulation Monte Carlo (DSMC) method[7–9] of Bird, which provides a numerical technique applicable for continuum to free-molecule flows; however, it is normally applied to the more rarefied flow regimes to minimize the computing requirements. Furthermore, it has been demonstrated[9–10] that the DSMC method permits the realistic simulation of flows with vortices.

DSMC simulations of rarefied hypersonic flows about spheres[11] show that the calculated sphere drag agrees well with measured wind-tunnel values. Furthermore, these calculations show that there are no vortices in the wake for freestream Knudsen numbers between 0.08 and 0.009. Navier-Stokes calculations for similar flow conditions[12] agree well with the experimental drag, but predict a steady vortex in the wake at a freestream Knudsen number of 0.009. Such discrepancies highlight the importance of using a particle simulation method such as DSMC to establish a data base for isolating the features of wake flows under conditions where rarefaction effects are significant. Recent DSMC simulations[13] of hypersonic flows about a 70-deg blunt cone show that a stable vortex exists in the base region for freestream Knudsen numbers between 0.01 and 0.001. For a freestream Knudsen number of 0.03, no vortex is observed.

The present paper is an extension of the work of Ref. 13, where the effects of surface temperature, size of corner radius, and the inclusion of an afterbody sting on the near-wake structure are investigated.

Computational Method and Boundary Conditions

The DSMC method[7–9] is used for the present calculations. The method and requirements for application of DSMC have been presented in previous publications[2,3] and are not repeated here.

The computational domain used for the calculations is large enough to capture most of the body disturbance at the upstream and side boundaries. Thus, freestream conditions are specified at these boundaries. The flow at the downstream outflow boundary is supersonic, and vacuum conditions are specified.

The flowfield was divided into eight regions, and a fine grid resolution was used for cells in the wake regions. The cell size in the forebody regions was of the order of half the local mean free path, except near the surface for case 3, where the cell size was of the order of the local mean free path. The cell size in the wake regions was much less than one-third the local mean free path. Furthermore, four subcells per cell were employed in all regions. Steady state was assumed when the number of simulated molecules in each region achieved a constant value (fluctuation within 0.2%). The average number of simulated molecules in a cell was 20 at steady state. The final results were obtained through a time-averaged solution over a large number of time steps.

The molecular collisions are simulated by the variable hard sphere (VHS) molecular model. This model employs the simple hard-sphere angular scattering law so that all directions are equally possible for the postcollision velocity in the center-of-mass frame of reference. However, the collision cross section is a function of the relative energy in the collision. The freestream viscosity and mean free path are evaluated using the VHS collision model with $T_{\text{ref}} = 300$ K, $d_{\text{ref}} = 4.07 \times 10^{-10}$ m, and $\bar{s} = 0.75$. Energy exchange between the translational and internal modes is modeled by the Larsen-Borgnakke statistical model[14] with a rotational relaxation number of 5.

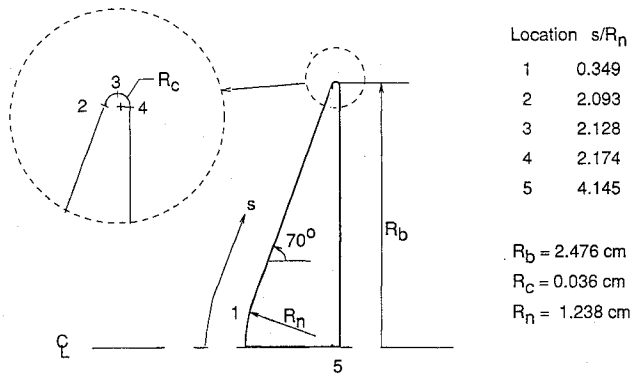

Fig. 1 Blunt-cone configuration.

Freestream and Wall Conditions

The freestream conditions considered for the nitrogen gas are attainable in the SR3 low-density tunnel[15] at the Centre National de la Recherche Scientific (CNRS), and are listed in Table 1. The model size selected is such that it can be tested in existing low-density hypersonic tunnels. The freestream parameters along with selected results are summarized in Table 2. The freestream mean free path is based on the VHS model, and it is calculated from the relation (see Ref. 8)

$$\lambda_\infty = \frac{(T_\infty / T_{\text{ref}})^\omega}{\sqrt{2} n_\infty \sigma_{\text{ref}} (2-\omega)^\omega \Gamma(2-\omega)} \tag{1}$$

$$\omega = \bar{s} - \tfrac{1}{2} \tag{2}$$

The gas-surface interaction is assumed to be diffuse with full thermal accommodation, and the surface temperature is assumed to be constant at 300 K. Because of the relatively low total temperature, the DSMC simulations model the nitrogen flow as a nonreacting gas with energy exchange between rotational and translational modes.

Results and Discussion

DSMC simulations were performed for three low-density wind-tunnel test cases (Table 1), and special attention has been focused on the near-wake structure to investigate whether or not a stationary vortex exists in the wake. In addition, a parametric study is performed for case 2 to investigate the effects of surface temperature, corner radius, and afterbody sting on the near-wake structure and the surface quantities. The 70-deg blunt-cone configuration is shown in Fig. 1.

Forebody Flow Structure

The effects of rarefaction on the forebody flow structure are clearly evident from Fig. 2, where the density profiles along the stagnation streamline are presented for three flow conditions. For cases 1 and 2 ($Kn_\infty = 0.03$ and 0.01, respectively), the density profiles show that the shock wave is very diffuse. However, for case 3, where $Kn_\infty = 0.001$, the density profile indicates the formation of a distinct yet thick shock wave. Near the stagnation point, a substantial density increase occurs. This is characteristic of hypersonic flows about cold blunt surfaces.

Wake Structure

Selected contours of nondimensional density ρ/ρ_∞, translational and internal temperatures, and Mach number, as well as streamlines, are shown in Figs. 3 and 4 for cases 1 and 3, respectively. The density contours for case 1 ($Kn_\infty = 0.03$) show (Fig. 3a) that the density rises gradually as the flow approaches the blunt body, further showing the diffuse nature of the shock wave that is characteristic of highly rarefied flows. Similar behavior has been observed for case 2. The density in the near wake for all three cases is less than 40% of the freestream value (Figs. 3a and 4a for cases 1 and 3 only). The density even drops below 10% of the freestream value in a region near the base, and this zone of very low density increases in size as the freestream Knudsen number increases. Figure 3b shows that there is substantial thermal nonequilibrium in the entire wake region of case 1. For case 3, most of the wake region is in thermal equilibrium (Fig. 4b). There is a small region near the base where the flow remains in thermal nonequilibrium. In addition to these thermal effects, a substantial portion of the wake flow in the base region is subsonic (Figs. 3c and 4c), and the extent of this subsonic region increases with decreasing freestream Knudsen number.

The streamlines for case 1 show that the flow is attached to the surface and there is no evidence of flow separation (Fig. 3d). This is expected because of the rarefied flow condition ($K_n = 0.03$ and $Re_\infty = 768$). However, for cases 2 and 3 the flow separates beyond the corner on the base of the body, and a stable vortex forms in the base region of the wake (Fig. 4d). It can also be inferred from these results that the separation point moves closer to the body corner with decreasing freestream Knudsen number.

The wake stagnation point is generally defined for separated flows as the location of a point in the wake where the flow reattaches and the flow velocity is zero. For axisymmetric separated flow, this point lies on the symmetry axis of the wake where the axial velocity is zero. The effect of rarefaction on the location of the wake stagnation point is shown in Fig. 5. The wake stagnation point moves toward the rear stagnation point with increasing freestream Knudsen number and finally coincides with the rear stagnation point for attached

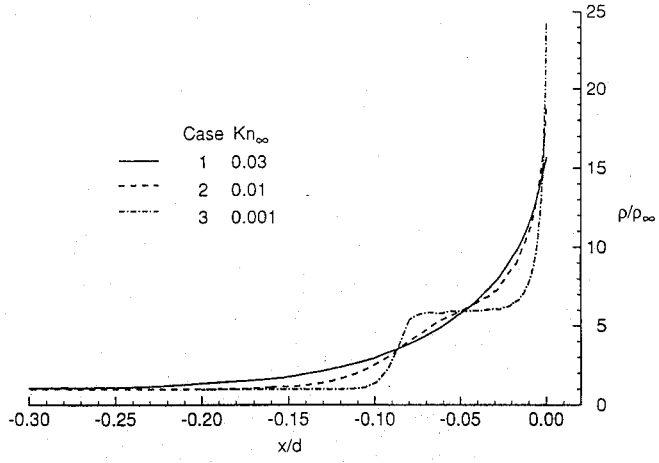

Fig. 2 Effect of rarefaction on stagnation streamline flow.

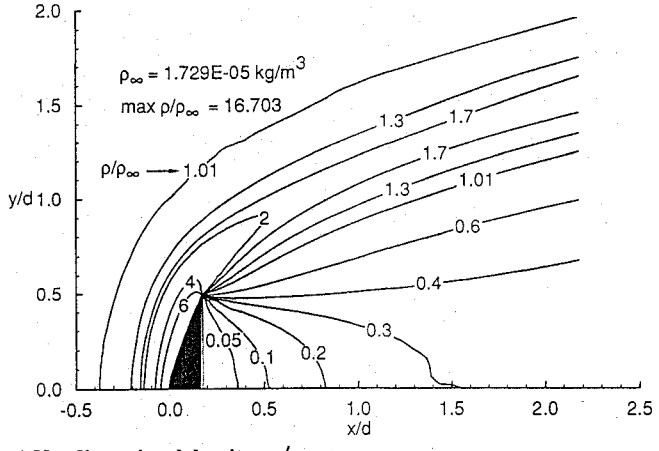

a) Nondimensional density, ρ/ρ_∞

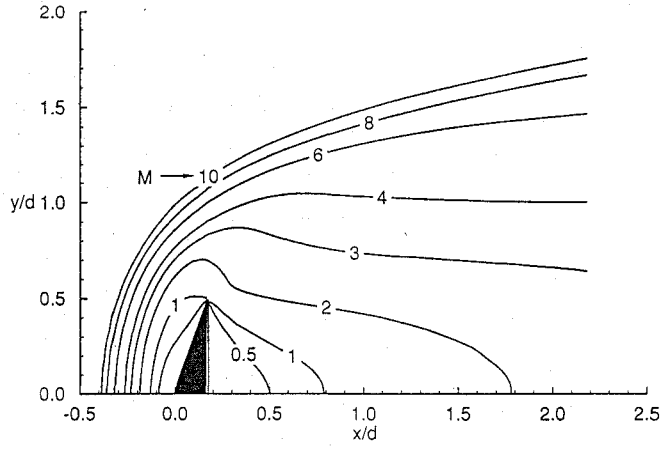

b) Translational and internal temperatures

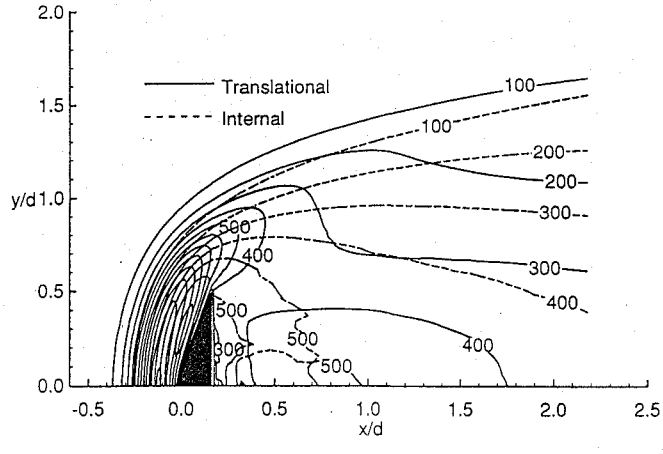

c) Mach number

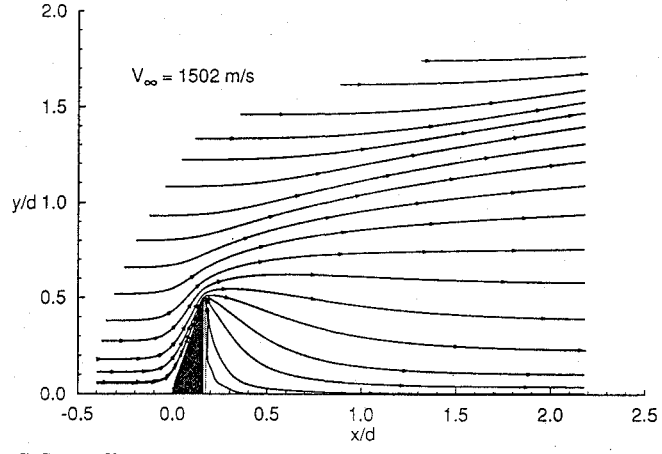

d) Streamlines

Fig. 3 Selected contours and streamlines (case 1, $Kn_\infty = 0.03$).

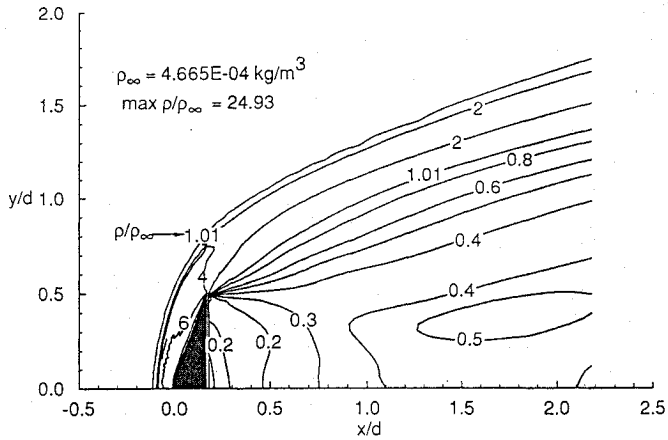

a) Nondimensional density, ρ/ρ_∞

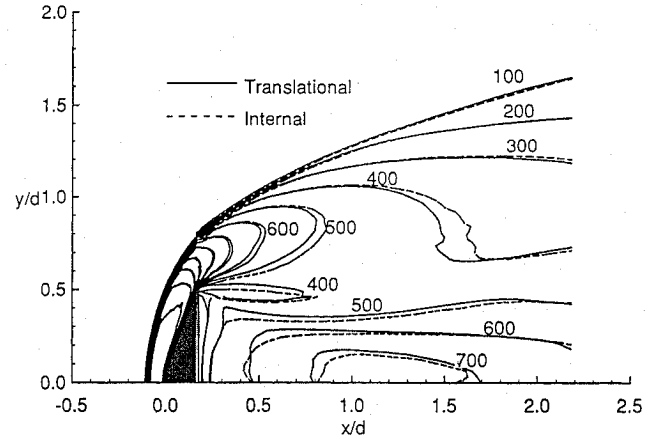

b) Translational and internal temperatures

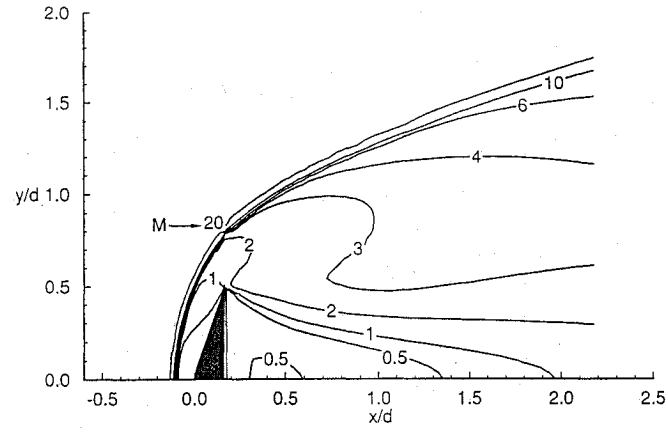

c) Mach number

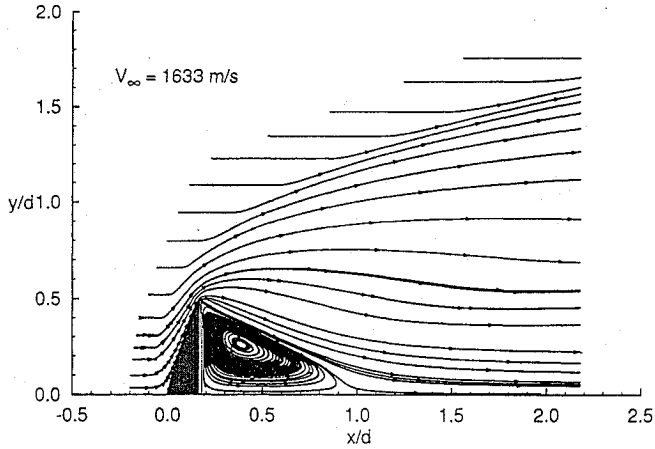

d) Streamlines

Fig. 4 Selected contours and streamlines (case 3, $Kn_\infty = 0.001$).

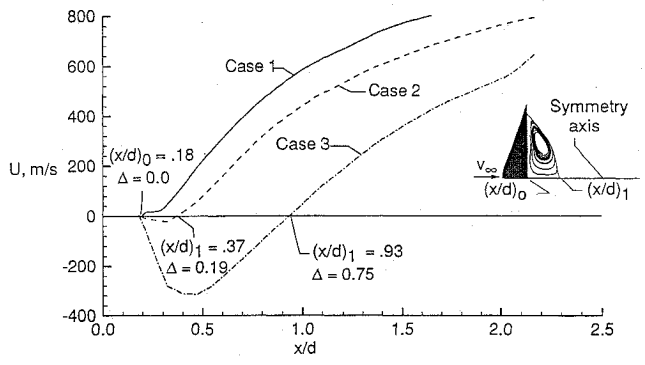

Fig. 5 Axial velocity along symmetry axis.

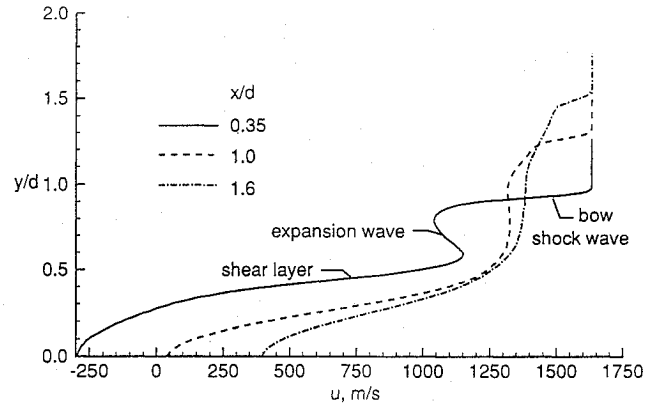

Fig. 6 Axial velocity profiles normal to wake symmetry axis (case 3, $Kn_\infty = 0.001$).

flow. Therefore, the size of the vortex (Δ) increases with decreasing rarefaction.

Figure 6 presents the axial velocity variation in the radial direction at three different axial locations in the wake for case 3. These results show that the shear-layer thickness changes very gradually with distance downstream of the base, and the leading-edge bow shock wave gradually becomes weak as the flow moves downstream in the wake. Also, the lip expansion fan diffuses in the streamwise direction, and there is no indication of any distinct wake compression wave. The wake features observed for case 3 become more diffused, and some aspects are no longer evident for the more rarefied cases. The lip expansion fan merges gradually with the shear layer and bow shock as the freestream Knudsen number increases.

Effect of Surface Temperature on Wake

Three surface temperature values (T_w = 100, 300, and 600 K) were considered for case 2 to investigate the effect of wall temperature on the near-wake structure. It can been seen from Fig. 7a that the density in the wake decreases gradually with increase in the surface temperature. The density in the wake is less than 45% of the freestream value at T_w = 100 K, and even smaller for the higher wall temperatures. Figure 7b shows that thermal nonequilibrium persists in the entire wake region for all three surface temperatures. Further, the translational and the internal temperature values in the wake increase with increasing surface temperature.

Figure 7c presents the velocities in the wake along the symmetry axis for case 2 for three different surface temperatures. As the surface temperature increases, the size of the vortex (Δ) decreases.

Effect of Corner Radius on Wake

Case 2 was investigated for three different corner radii (R_c/R_b = 0.0, 0.0145, and 0.05), where the value 0.0145 corresponds to

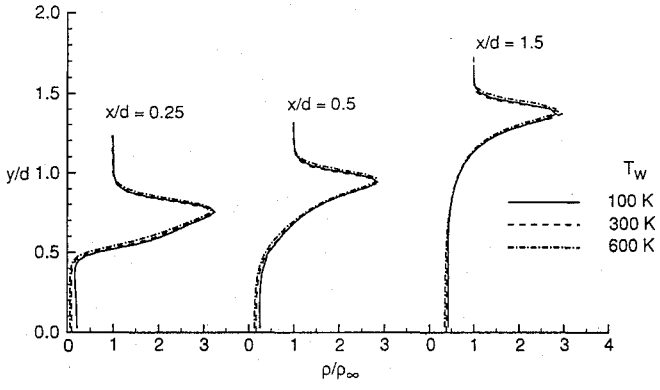

a) Wake density profiles

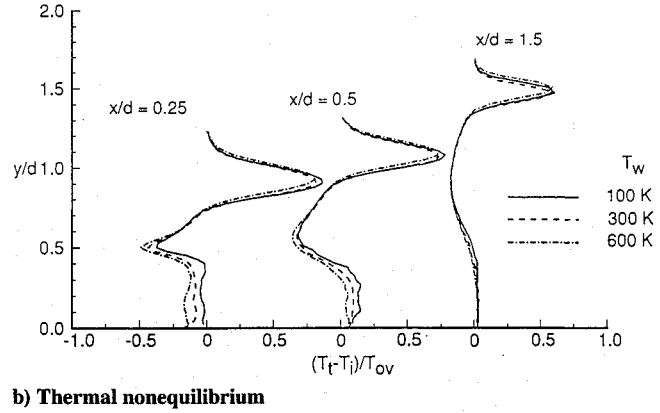

b) Thermal nonequilibrium

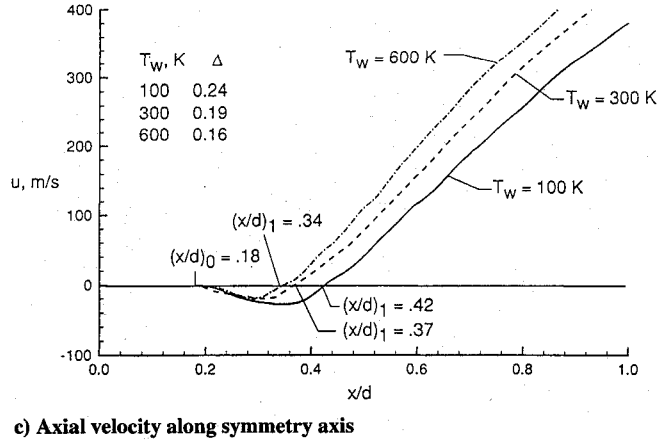

c) Axial velocity along symmetry axis

Fig. 7 Effect of surface temperature on wake structure (case 2, $Kn_\infty = 0.01$).

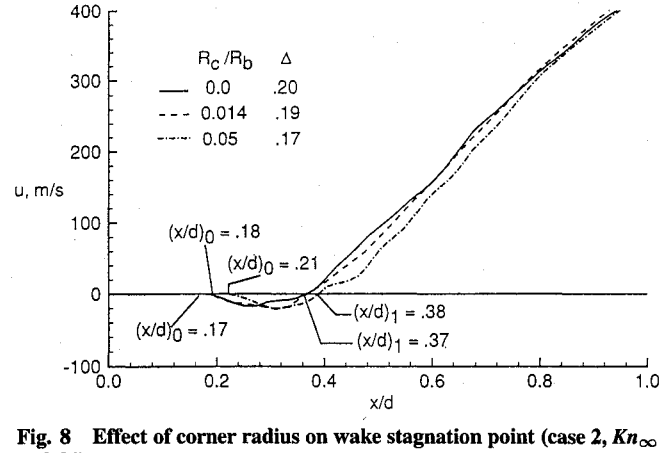

Fig. 8 Effect of corner radius on wake stagnation point (case 2, $Kn_\infty = 0.01$).

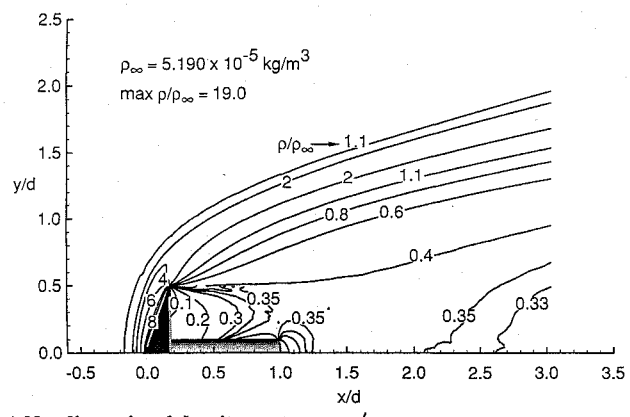

a) Nondimensional density contours, ρ/ρ_∞

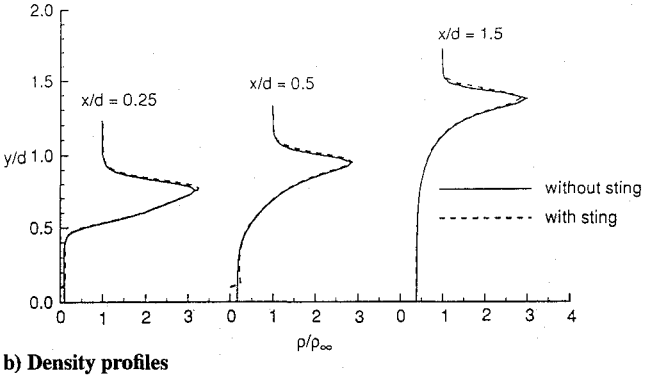

b) Density profiles

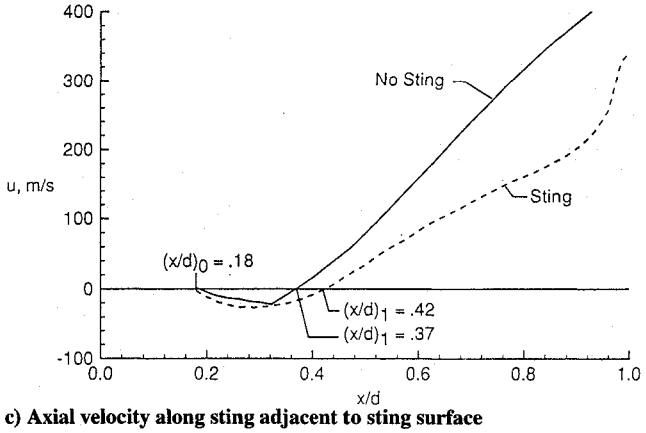

c) Axial velocity along sting adjacent to sting surface

Fig. 9 Effect of afterbody sting on wake structure (case 2, $Kn_\infty = 0.01$).

the Viking aeroshell[16] and the value 0.05 is the value under consideration for the Mars environmental survey (MESUR) probes.[17] It is inferred from these calculations that the density in the wake remains insensitive to the change of the corner radius except in the near-base region. The effect of the corner radius on the location of the wake stagnation point is shown in Fig. 8. The size of the vortex (Δ) is 15% smaller for $R_c/R_b = 0.05$ than for the sharp corner ($R_c/R_b = 0.0$).

Effect of Sting on Wake

A sting of radius 0.5 cm and length of 4.055 cm was attached to the 70-deg blunt cone, and calculations were performed for case 2 to investigate the effect of a sting on the wake structure. The density in the wake still remains less than 40% of the freestream value (Fig. 9a). The influence of the sting on the density in the wake is very small, as shown in Fig. 9b. However, the size of the wake vortex (Δ) is 26% greater with the sting, as shown in Fig. 9c.

Surface Quantities

The surface pressure, skin-friction, and heat-transfer coefficients are presented in Fig. 10 for the three flow conditions. The results are

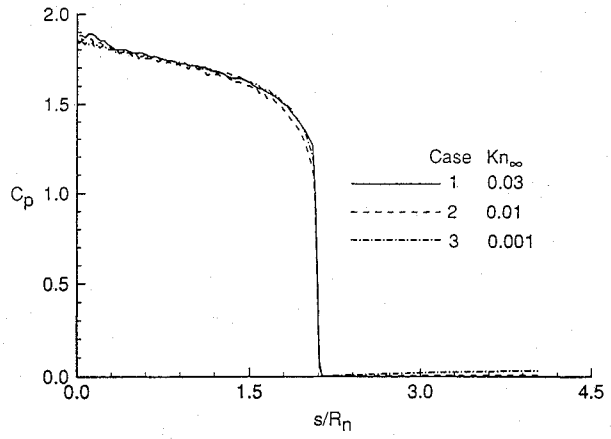

a) Pressure coefficient

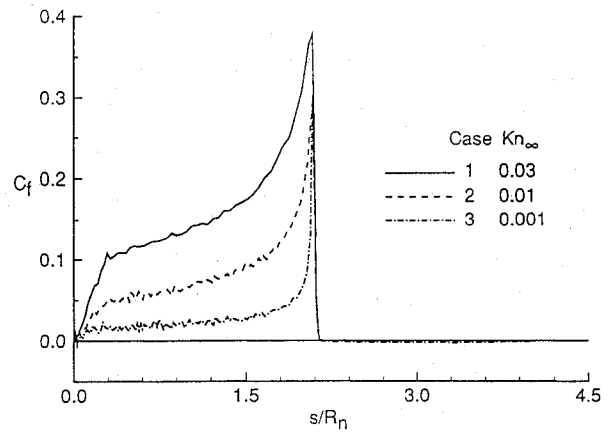

b) Skin-friction coefficient

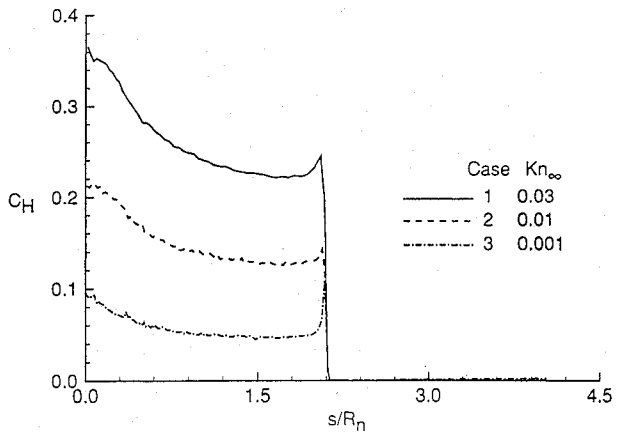

c) Heat-transfer coefficient

Fig. 10 Effect of rarefaction on surface quantities.

shown as a function of the nondimensional distance s/R_n along the surface, measured from the forebody stagnation point. The pressure coefficient is rather insensitive to the rarefaction effects (Fig. 10a), whereas the skin-friction and heat-transfer coefficients are very sensitive, as shown in Figs. 10b and 10c. The expansion of the flow about the aft corner for case 3 causes the maximum heat transfer to be at that point, rather than at the stagnation point (Fig. 10c). The base values of the surface pressure, skin friction, and heat-transfer coefficients are very small compared with those on the forebody surface for all three cases.

Figure 11 shows the effect of surface temperature on the heat-transfer coefficient for case 2. The pressure coefficient remains insensitive to the variation of the surface temperature, whereas the heat-transfer coefficient decreases with an increase in the surface temperature as expected.

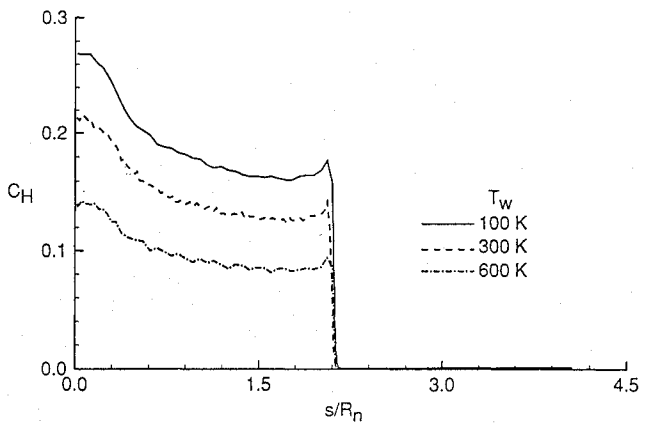

Fig. 11 Effect of surface temperature on heat-transfer coefficient (case 2, $Kn_\infty = 0.01$).

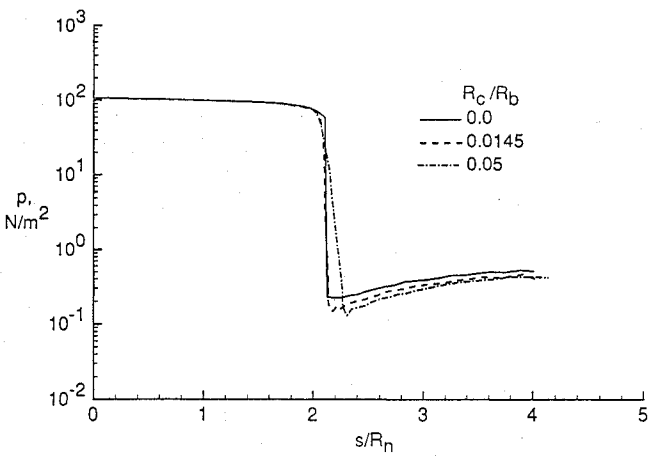

a) Pressure

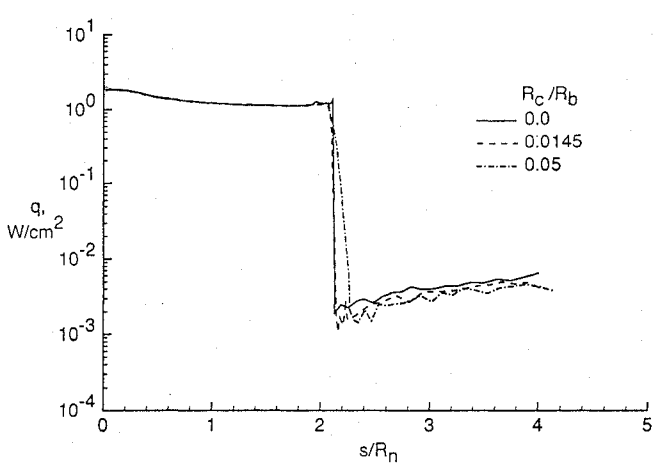

b) Heating rate

Fig. 12 Effect of corner radius on surface quantities (case 2, $Kn_\infty = 0.01$).

Figure 12 presents the dimensional pressure and heating distributions for case 2 in a format that highlights the magnitude of the surface quantities along the base surface. The base surface pressure (Fig. 12a) is of the order of 0.4 N/m^2, or 0.4% of the forebody stagnation value. The base heating rates are of the order of 40 W/m^2, or about 0.2% of the forebody stagnation value. Furthermore, with increasing rarefaction, the base pressure and heating become smaller fractions of their respective stagnation values. Also, as is shown in Fig. 12, the effect of the corner radius on the surface quantities is to produce somewhat higher pressure and heating with decreasing corner radius.

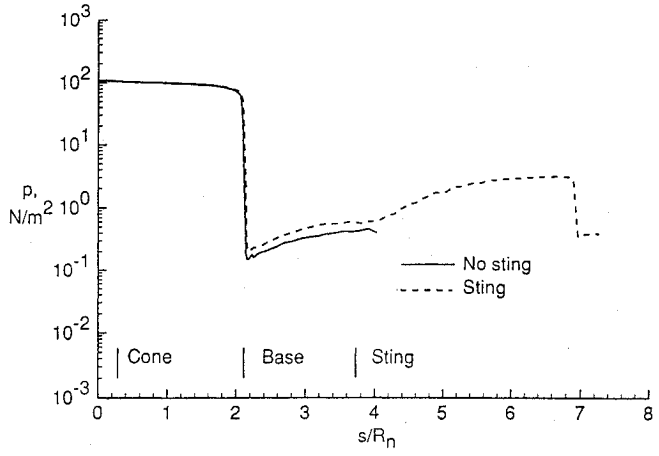

a) Pressure

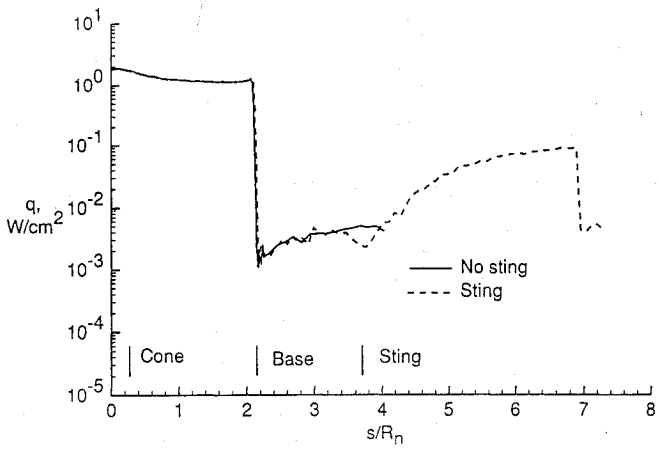

b) Heating rate

Fig. 13 Effect of sting on surface quantities (case 2, $Kn_\infty = 0.01$).

The effect of the sting on the surface quantities for case 2 is shown in Fig. 13. The presence of a sting does not influence the surface quantities in the forebody region; however, the sting has a small influence on the base pressure (Fig. 13a) and heating (Fig. 13b). The surface pressure, skin friction, and heat transfer increase gradually with distance along the sting, but the values remain small compared to the forebody values.

Concluding Remarks

Axisymmetric DSMC simulations of 70-deg blunt-cone flows have been performed for flow conditions attainable in existing low-density wind tunnels. For the range of freestream Knudsen numbers considered (0.03 to 0.001), the calculated results show that a stable vortex exists in the base region of the wake for freestream Knudsen numbers between 0.01 and 0.001 and the size of the vortex increases with decreasing freestream Knudsen number. The size of the vortex is moderately affected by the surface temperature, the corner radius, and the presence of a sting. For case 3, the maximum heat transfer occurs at the corner rather than at the stagnation point.

There is no formation of a lip separation shock or a distinct wake shock at these rarefied conditions. This is contrary to the behavior observed for blunt-body flows at continuum hypersonic conditions.

Acknowledgment

Support for V. K. Dogra by NASA Contract NAS1-19237 is gratefully acknowledged.

References

[1]Freeman, D. C., Powell, R. W., and Braun, R. D., "Manned Mars Aerobrake Vehicle Design Issues," International Aeronautical Federation, Paper 90-197, Oct. 1990.

[2]Moss, J. N., and Bird, G. A., "Direct Simulations of Transitional Flow for Hypersonic Re-Entry Conditions," *Thermal Design of Aeroassisted Orbital Transfer Vehicles*, edited by H. F. Nelson, Vol. 96, Progress in Astronautics and Aeronautics, AIAA, New York, 1985, pp. 113–139.

[3]Dogra, V. K., Moss, J. N., and Simmonds, A. L., "Direct Simulations of Aerothermal Loads for an Aeroassist Flight Experiment Vehicle," AIAA Paper 87-1546, June 1987.

[4]Celenligil, M. C., Moss, J. N., and Blanchard, R. C., "Three-Dimensional Rarefied Flow Simulations for the Aeroassist Flight Experiment Vehicle," *AIAA Journal*, Vol. 29, No. 1, Jan. 1991, pp. 52–57.

[5]Feiereisen, W. J., and McDonald, J. D., "Three Dimensional Discrete Particle Simulation of an AOTV," AIAA Paper 89-1711, June 1989.

[6]Gnoffo, P. A., Price, J. M., and Braun, R. D., "On the Computation of Near Wake, Aerobrake Flowfields," *Journal of Spacecraft and Rockets*, Vol. 29, No. 2, 1992, pp. 182–189.

[7]Bird, G. A., *Molecular Gas Dynamics*, Clarendon Press, Oxford, 1976.

[8]Bird, G. A., "Monte Carlo Simulation in Engineering Context," *Rarefied Gas Dynamics*, edited by Sam S. Fisher, Vol. 74, Part I, AIAA, New York, 1981, pp. 239–255.

[9]Bird, G. A., "Direct Simulation of Gas Flows at the Molecular Level," *Communications in Applied Numerical Method*, Vol. 4, No. 2, 1988, pp. 165–172.

[10]Moss, J. N., Price, J. M., and Chun, C. H., "Hypersonic Rarefied Flow about a Compression Corner—DSMC Simulation and Experiment," AIAA Paper 91-1313, June 1991.

[11]Dogra, V. K., Moss, J. N., Wilmoth, R. G., and Price, J. M., "Hypersonic Rarefied Flow Past Spheres Including Wake Structure," AIAA Paper 92-0495, Jan. 1992.

[12]Jain, A. C., and Dahm, W. K., "Hypersonic Merged Layer Blunt Body Flows with Wakes," *Rarefied Gas Dynamics*, edited by Alfred E. Beylich, VCH Weinheim, 1991, pp. 578–587.

[13]Dogra, V. K., Moss, J. N., Wilmoth, R. G., and Price, J. M., "DSMC Simulations of Hypersonic Low-Density Flow about an ASTV Including Wake Structure," *Rarefied Gas Dynamics: Space Science and Engineering*, edited by B. D. Shizgal and D. P. Weaver, Vol. 160, Progress in Astronautics and Aeronautics, AIAA, Washington, 1994.

[14]Borgnakke, C., and Larsen, P. S., "Statistical Collision Model for Monte Carlo Simulation of Polyatomic Gas Mixture," *Journal of Computational Physics*, Vol. 18, No. 4, 1975, pp. 405–420.

[15]Allegre, J., "The SR3 Low Density Wind-Tunnel. Facility Capabilities and Research Development," AIAA Paper 92-3972, July 1992.

[16]Blanchard, R. C., and Walberg, G. D., "Determination of the Hypersonic Continuum/Rarefied Flow Drag Coefficient of the Viking Lander Capsule Aeroshell from Flight Data," NASA TP-1793, Dec. 1980.

[17]Tauber, M., Henline, W., Chargin, M., Papadopoulos, P., Chen, Y., Yang, L., and Hamm, K., "Mesur Probe Aerobrake Preliminary Design Study," AIAA Paper 92-2952, July 1992.